2-1-2020

A characterization of Gaucher iPS-derived astrocytes: Potential implications for Parkinson's disease

Elma Aflaki
National Institutes of Health

Barbara K Stubblefield
National Institutes of Health

Ryan P McGlinchey
National Institutes of Health

Benjamin McMahon
National Institutes of Health

Daniel S Ory
Washington University School of Medicine in St. Louis

See next page for additional authors

Neurobiology of Disease 134 (2020) 104647

Contents lists available at ScienceDirect

Neurobiology of Disease

journal homepage: www.elsevier.com/locate/ynbdi

A characterization of Gaucher iPS-derived astrocytes: Potential implications for Parkinson's disease

Elma Aflaki[a], Barbara K. Stubblefield[a], Ryan P. McGlinchey[b], Benjamin McMahon[a], Daniel S. Ory[c], Ellen Sidransky[a,*]

[a] Section of Molecular Neurogenetics, National Human Genome Research Institute, NIH, Bethesda, MD 20892, United States of America
[b] Laboratory of Protein Conformation and Dynamics, National Heart Lung and Blood Institute, NIH, Bethesda, MD 20892, United States of America
[c] Department of Medicine, Washington University School of Medicine, St. Louis, MO 63110, United States of America

ARTICLE INFO

Keywords:
Parkinson's disease
Gaucher disease
Astrocytes
Induced pluriopotent stem cells
Glucocerebrosidase
GBA1
Alpha-synuclein

ABSTRACT

While astrocytes, the most abundant cells found in the brain, have many diverse functions, their role in the lysosomal storage disorder Gaucher disease (GD) has not been explored. GD, resulting from the inherited deficiency of the enzyme glucocerebrosidase and subsequent accumulation of glucosylceramide and its acylated derivative glucosylsphingosine, has both non-neuronopathic (GD1) and neuronopathic forms (GD2 and 3). Furthermore, mutations in *GBA1*, the gene mutated in GD, are an important risk factor for Parkinson's disease (PD). To elucidate the role of astrocytes in the disease pathogenesis, we generated iAstrocytes from induced pluripotent stem cells made from fibroblasts taken from controls and patients with GD1, with and without PD. We also made iAstrocytes from an infant with GD2, the most severe and progressive form, manifesting in infancy. Gaucher iAstrocytes appropriately showed deficient glucocerebrosidase activity and levels and substrate accumulation. These cells exhibited varying degrees of astrogliosis, Glial Fibrillary Acidic Protein (GFAP) up-regulation and cellular proliferation, depending on the level of residual glucocerebrosidase activity. Glutamte uptake assays demonstrated that the cells were functionally active, although the glutamine transporter EEAT2 was upregulated and EEAT1 downregulated in the GD2 samples. GD2 iAstrocytes were morphologically different, with severe cytoskeletal hypertrophy, overlapping of astrocyte processes, pronounced up-regulation of GFAP and S100β, and significant astrocyte proliferation, recapitulating the neuropathology observed in patients with GD2. Although astrocytes do not express α-synuclein, when the iAstrocytes were co-cultured with dopaminergic neurons generated from the same iPSC lines, excessive α-synuclein released from neurons was endocytosed by astrocytes, translocating into lysosomes. Levels of aggregated α-synuclein increased significantly when cells were treated with monomeric or fibrillar α-synuclein. GD1-PD and GD2 iAstrocytes also exhibited impaired Cathepsin D activity, leading to further α-synuclein accumulation. Cytokine and chemokine profiling of the iAstrocytes demonstrated an inflammatory response. Thus, in patients with *GBA1*-associated parkinsonism, astrocytes appear to play a role in α-synuclein accumulation and processing, contributing to neuroinflammation.

1. Introduction

Gaucher disease (GD) is a lysosomal storage disorder caused by mutations in *glucocerebrosidase 1 (GBA1)* gene, resulting in the deficiency of the enzyme glucocerebrosidase (GCase) and the accumulation of the glycolipid substrates glucosylceramide and glucosphingosine. GD is categorized into three types. In type 1 GD, the most common form, there is, by definition, no CNS involvement. Type 2, the acute neuronopathic form of GD (GD2) manifests in infancy, while chronic neuronopathic GD (GD3) may commence at any age. More recently, it has been established that patients with Parkinson's disease (PD) or the related disorder dementia with Lewy bodies (DLB) are more likely to carry a mutation in *GBA1* compared to controls (Nalls et al., 2013; Sidransky et al., 2009).

GD is primarily a disorder of the reticuloendothelial system, where lipid-laden macrophages contribute to the hematological, visceral and skeletal manifestations. However, much less is known about the pathogenesis of the brain involvement in neuronopathic forms of GD. Autopsy studies in patients with GD2 describe rare perivascular deposition of Gaucher macrophages, but unlike other lysosomal storage

* Corresponding author at: Section on Molecular Neurogenetics Medical Genetics Branch, National Human Genome Research Institute, NIH, Building 35, Room 1E623, 35 Convent Drive, MSC 3708, Bethesda, MD 20892-3708, United States of America.
E-mail address: sidranse@mail.nih.gov (E. Sidransky).

https://doi.org/10.1016/j.nbd.2019.104647
Received 14 August 2019; Received in revised form 14 October 2019; Accepted 23 October 2019
Available online 10 November 2019

disorders affecting the brain (Phatnani and Maniatis, 2015), very little CNS storage is observed (Lee, 1982). The most consistent finding has been significant neuronal loss with astrogliosis in cortical layer IV and in the hippocampal CA 2–4 regions. (Wong et al., 2004). These findings suggest a possible role of astrocytes in this disorder.

To date, most research on the neuropathology of Gaucher disease has focused on neurons, and the role of non-neuronal cells like astrocytes has remained unexplored. Recently, astrocytes have received increased attention in different neurodegenerative disorders (Phatnani and Maniatis, 2015). There is evidence to suggest that disruption in astrocyte function and biology might even contribute to neuronal degeneration in dopaminergic neurons (Du et al., 2018; Segura-Aguilar, 2015).

Astrocytes are the most abundant cells in the brain, and consequently, play pivotal roles in CNS homeostasis, including synaptic glutate acid uptake (Halassa et al., 2007), and providing nutrient support for neurons (Belanger and Magistretti, 2009). Astrocytes regulate synaptic transmission (Allen, 2014) and water transport within the brain (Eid et al., 2005). In addition, they produce different neurotrophic molecules such as glial-derived neurotrophic factor (GDNF), which is particularly important for the development and survival of dopaminergic neurons (Lin et al., 1993). Moreover, reactive astrocytes effectively phagocytose dead cells and protein aggregates like α-synuclein (α-syn) in synapses (Chung et al., 2013). Abnormal deposition of α-syn contributes to the pathogenesis of PD, and aggregated forms of α-syn are a major component of Lewy bodies. While astrocytes express extremely low levels of α-syn, some studies in both PD and DLB have shown the presence of aggregated α-syn in astrocytes and oligodendrocytes (Braak et al., 2007; Tu et al., 1998). However, the mechanisms responsible for the transfer of secreted α-syn from neurons to astrocytes and their neuro-inflammatory responses remain unclear.

To better understand the role of astrocytes in GD and GD-associated PD, we differentiated induced pluripotent stem cells (iPSCs) from patients with GD1 (with or without PD) and GD2 into functional astrocytes (referred to as iAstrocytes). We found that GD2 iAstrocytes show global impairments, consistent with the neuropathology noted in patient brains. We also report that in both GD2 and GD1-PD, α-syn released from neurons is endocytosed by astrocytes and translocates into lysosomes, indicating that these cells may play a role in PD pathogenesis.

2. Materials and methods

2.1. Differentiation of iPSCs into astrocytes

iPSCs were produced from three controls (two adults and one infant), five patients with GD1 (two who also had PD), with genotypes N370S/N370S or N370S/c.84insG (two colonies were evaluated, GD1–2/1 and GD1–2/2) and a patient with GD2 with genotype L444P/IVS2 + 1G > A (two different colonies were evaluated,GD2/1 and GD2/2) as previously described (Aflaki et al., 2016) (Table 1). In some experiments two different colonies from same line were used, and these are noted with a slash. To generate neuronal progenitor cells (NPCs), the iPSCs were detached and cultured in AggreWell 800 microwell culture plates (Stem Cell Technology) for 5 days. EBs were then plated onto Matrigel-coated plates for 6 days. After the appearance of typical neural tube-like rosettes, they were detached using STEMdif Neuronal Rosette Selection media (Stem Cell Technology) for differentiation into NPCs. Then differentiation to iAstrocytes was performed by a modified published protocol (Serio et al., 2013). The NPCs were cultured in Advanced DMEM (AdDMEM)/F12 supplemented media (ThermoFischer) with (1% N2 NeuroPlex™, 0.1% Gem21 NeuroPlex™ Supplement) (Gemini Bio-products), 1% nonessential amino acids, 1% GlutaMax and 20 ng/ml FGF-2, LIF and EGF (R&D Systems) for 2–3 weeks. After enrichment, cells were passaged and monolayer cultures were generated. Monolayer cultures were propagated in Advanced DMEM/F12 (ThermoFisher) supplemented with 1% N2 NeuroPlex™, 0.1% Gem21 NEUROPLEX™ Supplement, 1% nonessential amino acids, 1% GlutaMax, 20 ng/ml FGF-2 and EGF (R&D Systems) and passaged when confluent using Acutase (Millipore). Mature astrocytes were obtained by differentiating immature cells for 20 days with neurobasal medium (ThermoFisher) supplemented with 0.2% Gem21 NeuroPlex™, 1% nonessential amino acids, 1% GlutaMax and 5 ng/ml CNTF and BMP4 (R&D Systems) on Matrigel coated plates. After initially optimizing the differentiation of iPSCs into astrocytes, iPSCs were differentiated in two independent experiments and all assays were performed at least twice with astrocytes generated during each differentiation.

2.2. Immunocytochemistry

Cells were plated on glass chamber slides coated with Matrigel and fixed with 4% methanol free PFA (Electron Microscopy Sciences). Cells were blocked in PBS containing 0.1% saponin, 100 μM glycine, and 2% donkey serum, followed by incubation with the primary antibody (Table 2). They were washed and incubated with donkey anti-mouse, anti-rabbit or anti-chicken secondary antibodies and conjugated to Alexa-488, Alexa-555 or Alexa-643 (Invitrogen) (1:300). Cells were mounted with ProLong Gold Antifade or Diamond Antifade (Molecular Probes™) with or without DAPI, and *Z*-stack images were acquired with a Zeiss 880 META Laser Scanning Microscope. Images were acquired using a 63× Plan- NeoFluar lens (Zeiss).

2.3. GlcCer and GalCer analysis by mass spectrometry

Cell pellets generated from the cultured iPS-astrocytes were homogenized in water, spiked with internal standards (C17 S1P, *N*,*N*-dimethylpsychosine, GalCer(d18:1 8:0)), and extracted with methanol. One portion of the extract was used for quantification of GlcSph and GlcCer, using reverse-phase C18 columns for HPLC/MS/MS. The other portion was used for the determination of GlcSph as well as GlcCer using an HILIC column. The results were normalized to total protein.

2.4. Immunoblotting

iPS-derived astrocytes were harvested and sonicated at 4 °C in RIPA buffer (50 mm Tris-HCl, pH 7.4, 150 mm NaCl, 0.5% Na-deoxycholate,

Table 1
iPSC lines used and their *GBA1* genotypes.

Line	*GBA1* Genotype
Control-1	wt/wt
Control-2 (2 colonies available)	wt/wt
GD1–1 (type 1 GD)	N370S/N370S (p.N409S/p.N409S)
GD1/PD-1 (type 1 GD and PD)	N370S/N370S (p.N409S/p.N409S)
GD1–2 (2 colonies were used)	N370S/c.84insG (p.N409S/c.84insG)
GD1/PD-2 (2 colonies available)	N370S/c.84insG (p.N409S/c.84insG)
Infant control	wt/wt
GD2 (type 2GD-2 colonies used)	L444P/IVS2 + 1G > A (p.L483P/IVS2 + 1G > A)

Table 2
Antibodies used in this study.

Antibodies	Company	Cat#
S100β (anti-mouse) (1:500)	Sigma	HPA015768
GFAP (anti-chicken) (1:500)	Abcam	ab4674
CD44 (anti-rabbit) (1:400)	Abcam	ab189524
Aquaporin-4 (anti-rabbit) (1:250)	Abcam	ab4164182
Ki67(anti-rabbit) (1:400)	Abcam	ab92742
Rab5 (anti-rabbit) (1:300)	Cell signaling Technology	3547
Cathepsin D (anti-goat)(1:350)	R&D system	AF-1014
Lamp1 (anti-mouse) (1:500)	Hybrodoma	H4B4
GCase (anti-rabbit)(1:10,000)	In house	
EAAT1/EAAT2 (anti-rabbit) (1:250)	Abcam	Ab41751/ab41621
PSD95 (anti-mouse) (1:350)	Abcam	ab13552
Synapsin1 (anti-rabbit) (1:350)	Abcam	ab64581

0.1% SDS, Protease Inhibitor Cocktail (Roche) and 2× Phosphatase Inhibitor (Invitrogen). After quantification with BCA (ThermoFischer), 10 µg of the lysate was separated by Criterion™TGX™ SDS-PAGE Gel System (Bio-Rad) and transferred to Trans-Blot Turbo PVDF membranes (Bio-Rad). Blots were blocked in 1:1 PBS, Odyssey Blocking Buffer (Li-COR Bioscience) for 1 h at room temperature. The membrane was incubated in blocking buffer containing 0.1% Tween 20 (Sigma), and primary antibodies including: EAAT1 and EAAT2 (Abcam), Rab7 and Rab11 (Cell Signaling), and α-synuclein (Santa Cruz Biotechnology) overnight at 4 °C, followed by three 15 min washes. The membrane was incubated in IRDye 680RD or IRDye 800RD secondary antibody 1:10,000 (Li-COR Bioscience) for 1 h at room temperature. The blots were imaged using an Odyssey imaging system (Li-CORE Bioscience) and quantified using Image Studio Lite software (Li-CORE Bioscience). To detect total protein in the blot, the membrane was stained with Revert total protein stain (Li-CORE Bioscience) and was imaged using Image Studio Lite Software (Li-CORE Bioscience).

2.5. GCase activity

iPS-derived astrocytes were lysed in citrate-phosphate extraction buffer (pH 4.2). To exclude activity from other non-lysosomal GCase, lysates were incubated with or without 100 µm conduritol-β-epoxide (CBE) (Sigma), an inhibitor specific for GBA1, for 30 min and the amount of uninhibited activity was subtracted from the total. Assay buffer (1 M 4-MU β-glu (Sigma) to a final concentration of 10 mM in citrate-phosphate buffer was added for 150 min at 37 °C. The reaction was halted using a stop solution (1 M NaOH and 1 M glycine) and fluorescence measured using a FlexStation3 plate reader (Molecular Devices), normalized to total protein.

2.6. Calcium assay

An equal number of iAstrocytes were cultured on Matrigel-coated black 96-well plates. Cells were incubated with 2.5 µM Fluo-4 AM and 0.02% Pluronic F127 detergent (Molecular Probes™) in HBSS buffer for 30 min at 37 °C. Then cells were washed with HBSS buffer and incubated for a further 30 min at 37 °C to allow de-esterification of intercellular AM esters. 3 µM ATP (Sigma) was added 30 s after reading the basal calcium level, and fluorescence (Ex/Em 494/516 nm) was measured kinetically for 3 min using a FlexStation 3 (Molecular Devices).

2.7. Cathepsin D activity

iAstrocytes were lysed in citrate-phosphate extraction buffer (pH 5.3) and Cathepsin D activity was measured using a Cathepsin D activity Fluorometric Assay Kit (Biovision). Fluorescence was measured (Ex/Em 328/460) using a FlexStation 3 (Molecular Devices) and normalized to total protein.

2.8. Glutamate uptake assay

iAstrocytes were plated on Matrigel-coated black 96-well plate for over 2 weeks at 37 °C. For the glutamate uptake assay (Serio et al., 2013), iAstrocytes were cultured in HBSS with 100 µM L-Glu (Sigma) for 30, 60 and 120 min and the concentration of L-Glu in the media was measured by using an Amplite Fluorimetric Glutamic Acid Assay Kit (ATT Bioquest). Fluorescence was measured (Ex/Em 571/585 nm) using FlexStation 3 (Molecular Devices). HBSS and L-Glu supplemented with 2 mM L-transpyrrolidine-2,4-dicarboxylic acid (Sigma) was used as a negative control and was assayed at 120 min. In addition, a CyQuant Cell Proliferation Assay (Molecular Probes™) was performed to obtain an indirect estimate of the number of cells per well. The data from the glutamate clearance assay was then normalized to the number of cells.

2.9. Protein expression and purification of α-synuclein

N-terminally acetylated α-synuclein was expressed in BL21(DE3) (O'Leary et al., 2018) using human α-syn (pRK172) (Jakes et al., 1994) and yeast NatB genes (Johnson et al., 2010). The α-synuclein sequence also contains a silent mutation (TAT) at residue 136 to avoid the spontaneous mutation of Tyr-to-Cys (Masuda et al., 2006). Purification was carried out as previously described (Pfefferkorn and Lee, 2010). Purity of α-syn was assessed by SDS-PAGE (NuPAGE 4–12% Bis-Tris, Invitrogen) and confirmed by mass spectrometry (NHLBI Biochemistry Core). Protein concentrations were determined using a molar extinction coefficient estimated on basis of amino-acid content: $\varepsilon 280\,\text{nm} = 5120\,\text{M}^{-1}\,\text{cm}^{-1}$. Purified proteins were aliquoted and stored at −80 °C until use.

2.10. Formation of fibrils

α-Synuclein was exchanged into pH 5 buffer (50 mM NaOAc, 20 mM NaCl) using a PD-10 column (GE Healthcare) and filtered through YM-100 filters (Millipore) prior to aggregation. Fibril formation was performed in microcentrifuge tubes (1.5-mL Protein LoBind tubes, cat. 022431081, Eppendorf) containing 1 mL solution ([α-syn] = 117 µM) with continuous shaking at 600 rpm at 37 °C for 3 days in a MiniMicro 980140 shaker (VWR).

2.11. Studies of α-synulein trafficking

iAstrocytes were cultured on coverslips coated with Matrigel. Cells were incubated with monomeric recombinant human α-syn (1–140) HiLyte™ Fluor 488 labeled (AnaSpec) for 24 h and 48 h in neurobasal medium (ThermoFischer) without Phenol Red (Invitrogen). The cells were washed 3 times with PB, and were fixed with chilled methanol for 1 min at 4 °C in order to stain for membrane proteins.

2.12. ELISA measurements

iAstrocytes were treated with monomeric (Ana Spec) and fibrillar α-syn for 48 h. They were then washed and incubated with neurobasal medium without Phenol Red for 24 h. After treatment, media were collected and kept at -80 °C for further analyses. Cells were lysed and equal amounts of protein were used for the ELISA according to the manufacturer's instructions (Abcam).

2.13. Measuring aggregated α-synuclein using Time-resolved Fluorescence Resonence Energy Transfer (RT-FRET)

iAstrocytes were treated with monomeric and fibrillar α-syn for

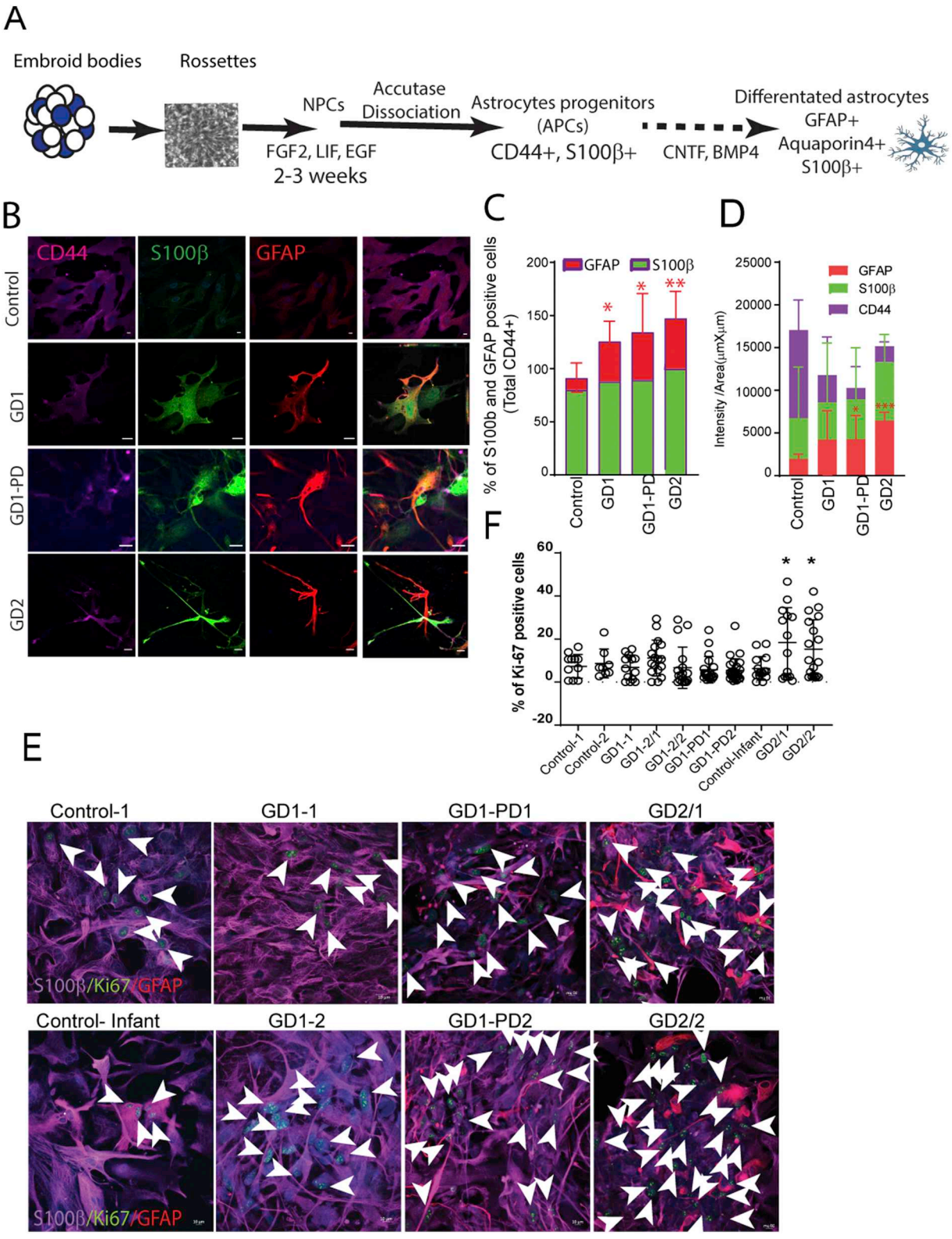

Fig. 1. Differentiation of iAstrocytes from GD or control iPSCs. (A) Generation of iAtrocytes from iPSCs. (B) iAstrocytes from Control, GD1 (with or without PD) and GD2 iPSCs were stained for astrocytes markers CD44 (purple), S100β (green) and GFAP (red) 1 week after exposure to CNTF and BMP4. (C) The.percentage of GFAP or S100β positive cells were measured in the CD44+ population derived from three independent differentiations. (D) Intensity of the GFAP and S100β per μm/area were measured using Black Zen software from three independent differentiations. (E) Astrogliosis was measured in iAstrocytes. iAstrocytes were stained for Ki-67 (green), S100β (purple and GFAP (red). Scale bars; 10 μm. (F) The percentage of Ki-67 positive nuclei was calculated (arrows show Ki-67 positive nuclei). Statistically significant differences were seen in iAstrocytes differentiated from both GD2 colonies compared to the infant control iAstrocytes: *$p = .04$ Graph represents data from three independent experiments. (For interpretation of the references to colour in this figure legend, the reader is referred to the web version of this article.)

48 h. The cells were washed, lysed and same amount of protein was used for the assay according to the manufacturer's instructions (Cisbio). Fluorescence was measured at 665 nm using the FlexStaion 3 (Molecular Devices).

2.14. Cytokine and chemokine profiling of iAstrocytes

iAstrocytes were incubated with or without endotoxin-free monomeric (AnaSpec) or fibrillar α-synuclein (10 μg) for 48 h in conditioned neurobasal medium without Phenol Red. After treatment, the conditioned medium was harvested and processed for cytokine and chemokine profiling using a Human Cytokine Array (R&D Systems). The array membranes were incubated with conditioned medium and the antibody cocktail overnight at 4 °C. After several washings, membranes were incubated with IRDye 800CW Streptoavidin (LICOR) and membranes were imaged and analyzed using the ImageStudioLite (LICOR).

2.15. Co-culture of iDA and iAstrocytes

To test the transmission of α-syn from iPS-derived dopaminergic neurons (iDA) to iAstrocytes, co-culture was performed. iDA neurons were differentiated from NPCs as previously described (Aflaki et al., 2016), using growth factors obtained from R&D Systems, unless otherwise noted. Briefly, neuronal induction medium I (DMEM/F12 supplemented with L-glutamine [2 mm], N2 supplement, BSA [1 mg/ml], Y27632 [10 μm; Tocris Bioscience], SB431542 [10 μm, Tocris Bioscience] and noggin [200 ng/ml]) was added to the NPCs for 3 days. The media was changed at day 4, withdrawing SB43152 and noggin and adding 200 ng/ml sonic hedgehog [SHH C24II], fibroblast growth factor-8a (FGF8a, 100 ng/ml), and ascorbic acid (200 μm; Sigma) for 10 days. Cells could then be passaged and were maintained in their final differentiation media (DMEM/F12 supplemented with L-glutamine [2 mm], N2 supplement, BDNF [20 μg/ml], and glial-derived neurotrophic factor [GDNF, 20 μg/ml]).

iDA cells were cultured in the lower compartment of a transwell system with a 0.4 μm pore size (Corning), and iAstrocytes were seeded in the insert. Cells were maintained in neurobasal medium without Phenol Red, serum free with 0.2% Gem21 NeuroPlex™. Then, neurons and astrocytes were lysed in RIPA buffer with protease and phosphate inhibitor, and were immunoblotted for α-synuclein.

2.16. Synaptogenesis

iDPA and iAstrocytes were co-cultured, and neurons were fixed and stained for PSD95 (1:300), Synapsin1 (1:250) and MAP2 (1:350), and imaged with an Airy 880 confocal microscope. The average number of PSD95 + /Synapsin1 + puncta were analyzed using Puncta analysis ImageJ software (Ippolito and Eroglu, 2010).

2.17. Statistical analysis

Statistical analyses were performed using GraphPadPrism 8.0 software. After optimizing the differentiation of iPSCs into astrocytes and all of the functional assays, iAstrocytes were differentiated from iPSCs in two independent experiments. After each differentiation, assays were perfomed in duplicate. Thus the presented data were pooled from four different experiments. Significance was determined by a Student's *t*-test. Data from two groups or > 2 independent variables were analyzed by ANOVA, followed by the Bonferroni post hoc test. Data are presented as mean values + / − SD. Significance levels between controls and patient macrophages were set when $p < .05$(*), $p < .01$(**), and $p < .001$(***) between different conditions.

3. Results

3.1. Initial phenotyping of the i-Astrocytes

Astrogliosis encompasses the spectrum of molecular, cellular and functional changes in astrocytes that occur in response to CNS injury (Sofroniew and Vinters, 2010). Different aspects of astrogliosis were evaluated in iAstrocytes generated from iPSC lines previously described by our group (Aflaki et al., 2014) (Table 1). iPSCs were differentiated into neuronal progenitor cells (NPCs), and then cultured in medium containing FGF2, LIF and EGF. Astrocyte progenitor cells (APCs) were differentiated from NPCs in the presence of EGF and FGF-2 (Fig. 1A). iAstrocytes were stained for CD44, a surface marker in astrocytes precursor cells (APCs), and both S100β and Glial Fiblirary Acidic protein (GFAP), were used as astrocyte markers. All iAstrocytes expressed CD44, while the percentage of the GFAP positive cells were higher in the GD iAstrocytes compared to controls (Fig. 1B, C) Control iAstrocytes had high levels of CD44, but low levels of GFAP (Fig. 1B, C). GD1 iAstrocytes showed increased levels of GFAP and some degree of cytoskeletal hypertrophy, reflecting mild to moderate astrogliosis. However, GD2 iAstrocytes demonstrated pronounced up-regulation of GFAP and S100β, severe cytoskeletal hypertrophy (Fig. 1B–D) and overlapping of astrocyte processes. These findings are indicative of diffuse astrogliosis.

Since the proliferation of astrocytes plays an important role in reactive astrogliosis, iAstrocytes were co-stained with the cell cycle marker Ki-67, along with the astrocyte markers S100β and GFAP. As shown in Fig. 1E, F, a significant increase in cell proliferation was observed in GD2 iAstrocytes, as reflected by the abundance of Ki-67 positive cells, which can occur with severe diffuse astrogliosis. Significant upregulation of GFAP, pronounced cytoskeletal hypertrophy, overlapping of cellular processes with their neighboring astrocytes, as well as astrocyte proliferation, all confirm severe and diffuse astrogliosis in the GD2 samples.

3.2. Gaucher iPS-Astrocytes show reduced glucocerebrosidase activity and levels

Glucocerebrosidase (GCase) protein levels and activity were analyzed in iAstrocytes kept in medium with CNTF and BMP4 for > 2 weeks. As anticipated, both GD1 and GD2 iAstrocytes showed correspondingly low levels of GCase protein (Fig. 2A, B). Furthermore, GD1 iAstrocytes showed the expected reduction in GCase activity (< 35% of control), whereas GD2 iAstrocytes had severely deficient (< 5% of control) GCase activity (Fig. 2C). Next, using mass spectrometry, levels of GlcCer and GlcSph were measured in iAstrocytes held in culture for 3 weeks in the presence of CNTP and BMP4. iAstrocytes from the subjects with GD1 with a parkinsonian phenotype showed 3–3.5 fold higher levels of GlcCer than control iAstrocytes. Cells from the two lines generated from the subject with GD2 had 3.5 and 5.6 fold elevations in GlcCer level compared to those from an infant control (Fig. 2D). Moreover GlcSph levels were significantly elevated in GD2 iAstrocytes (10–20 fold) (Fig. 2E), while GlcSph was barely detected in the iAstrocytes from the control infant. This marked elevation in GlcSph is consistent with levels measured in brain autopsy samples from patients with GD2 (Orvisky et al., 2002). Samples from one patient with GD1/PD also had elevated GlcSph.

3.3. iPSC-derived astrocytes are biologically functional

An important astrocyte markers is Aquaporin-4 (AQP-4), the predominant water channel expressed by astrocytes in the CNS. AQP-4 is highly expressed in the astrocyte's end-feet, which are protrusions in contact with blood vessels, and plays a pivotal role in regulating fluid homeostasis in the healthy CNS (Nielsen et al., 1997). iAstrocytes were stained for AQP-4 along with the astrocyte markers S100β and GFAP

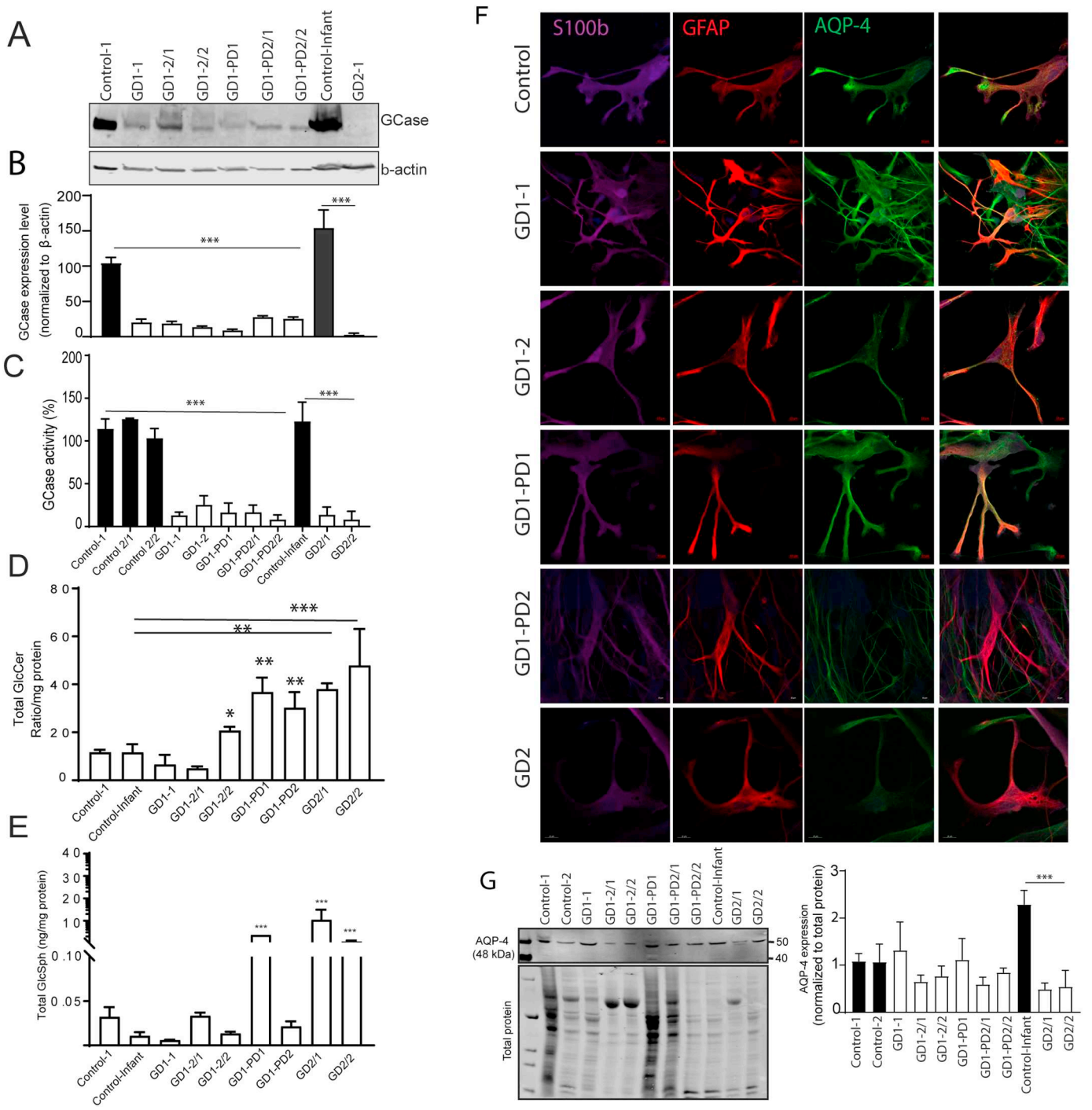

Fig. 2. iPS-derived astrocytes recapitulate the GD phenotype. (A) Western blot analysis of GCase in iAstrocytes from controls, GD1 (with or without PD) and GD2. β-actin used as a loading control. Data represents results from three independent experiments. (B) Quantification of the western blot shown in panel A. (C) GCase activity (percentage of control) in iAstrocytes. Graph represents data from two independent differentations. Each experiment was performed two times in triplicate for each differentiation. (D, E) GlcCer(C) [$*p = .04$, $**p = .006$; .0016;$***p = .0002$] and GluSph (D) [$***p = .0003$] levels measured in iAstrocytes using HPLC/MS/MS. Data reperesents pooled data from three independent experimenrs and each sample was analyzed in quadriplicates. (F) iAstrocytes were stained for Aqu4 (green), S100β (purple) and GFAP (red). Scale bars; 5 μm. (G) Western blot analysis was performed on samples obtained from two independent differentiations and Aquaporine 4 expression was normalized to total protein.

(Fig. 2F). Fig. 2G shows similar AQP-4 expression levels in control and GD1 iAstrocytes, while in GD2 iAstrocytes AQP-4 was reduced compared to the infant control and was not observed in the astrocyte endfeet.

Next, we performed an extracellular glutamate uptake study to evaluate astrocyte function. Extracellular glutamate uptake is critical for maintaining synaptic signaling and inhibiting excitotoxicity. EAAT2 (GLT-1) and EAAT1 (GlAST) are the primary astrocyte glutamate transporters (DeSilva et al., 2012). We found that EAAT2 localized on the surface of all samples except for the GD2 iAstrocytes (Fig. 3A), and EAAT2 protein levels were elevated in GD2 and GD1-PD iAstrocytes (Fig. 3C). Immunolabeling and confocal imaging revealed that EAAT1 is also expressed in iAstrocytes (Fig. 3B, C), although the levels of EAAT1 were reduced in the GD2 iAstrocytes. In addition, no difference was

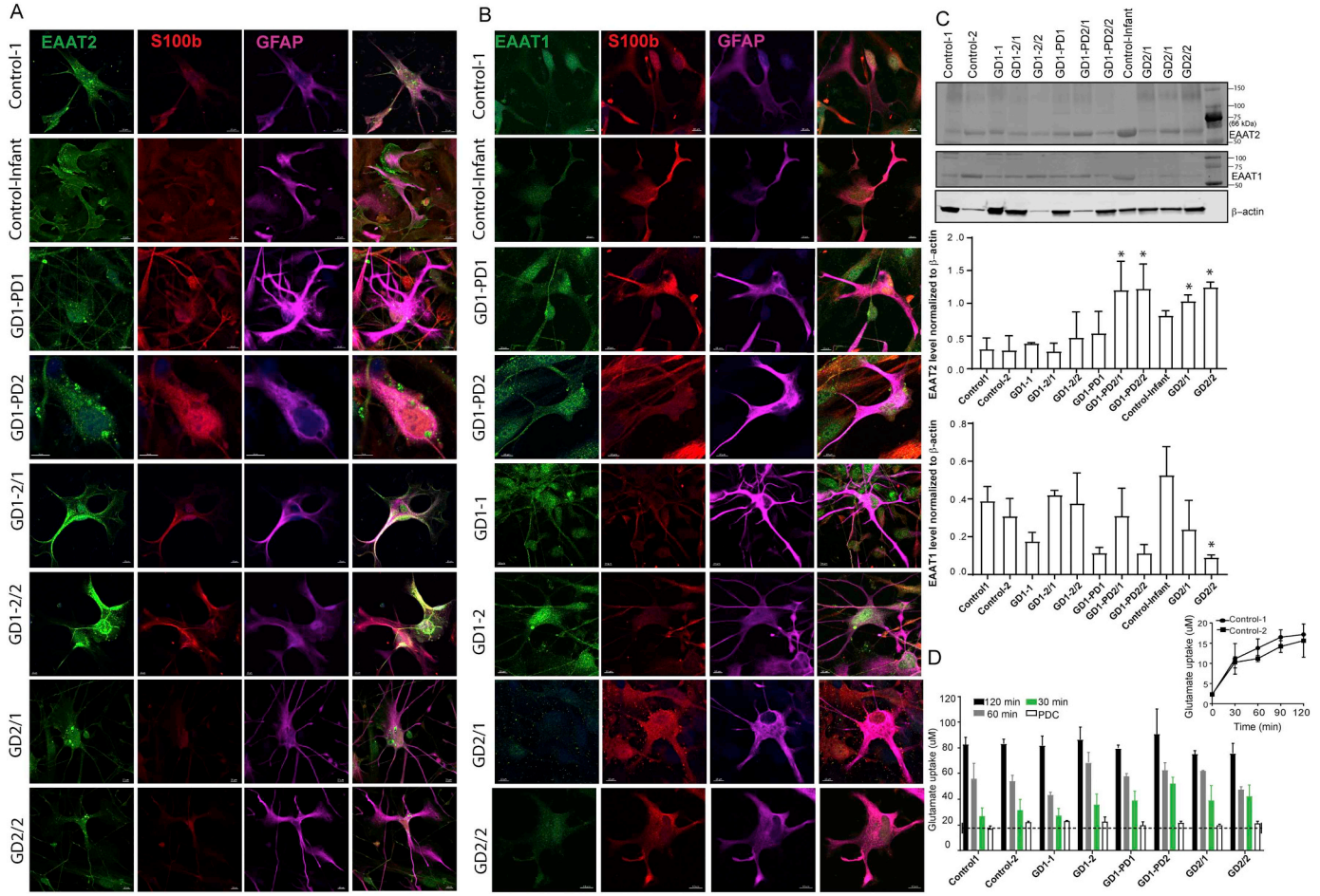

Fig. 3. Functional characterization of iAstrocytes. (A, B) iAstrocytes from subjects with GD1 (with or without PD) and GD2 were stained for EAAT2 and EAAT1 (A/B) (Green), S100β (red) and GFAP (purple). Scale bars = 5 μm. (C) Western blot analysis of EAAT2 (*p = .03; .02) and EAAT1(*p = .035) levels in iAstrocytes. β-actin is used as the loading control. Graphs show the quantification of the results as the ratio of EAAT2 (66 kDa) or EAAT1 to β-actin. Results from some iAstrocytes derived from two different colonies from the same fibroblast line are shown. Graphs represents pooled data from 4 experiments obtained from 2 independent differentiation. (D) L-glutamate uptake assay performed on iAstrocytes. iAstrocytes cleared L-glutamate in a time dependent manner. The uptake was blocked by the presence of 2 mM L-trans-pyrrolidine-2,4-dicarboxylic acid (PDC). Graph represents data from four independent experiments, each in triplicate. (For interpretation of the references to colour in this figure legend, the reader is referred to the web version of this article.)

observed between control and GD iAstrocytes with regard to the clearance of L-glutamate from the media in a time dependent manner. L-glutamate uptake was blocked by the glutamate uptake inhibitor, L-transpyrrolidine-2,4-dicarboxylic acid (PDC) (Fig. 3D) and was used as control for the assay.

3.4. Calcium signaling in response to ATP

Another important role of astrocytes is to respond to neurotransmitters released by neurons by increasing intracellular calcium (Zhang et al., 2016). We used Flou-4 AM, a calcium sensitive dye, to study whether iAstrocytes could respond to calcium signaling after the injection of 3 μM ATP. We found that control and GD1 (with or without PD) iAstrocytes responded to extracellular ATP, but the GD2 iAstrocytes did not (Fig. 4A). The area under curve also indicates a significant decrease in calcium signaling in response to ATP in GD2 iAstrocytes (Fig. 4B).

Next, we explored whether iAstrocytes promoted the formation of synapses. iAstrocytes were co-cultured with iDA derived form the same iPSC line for 5 weeks. The neurons were then stained for both the presynaptic protein synapsin 1 (Syn1) and a postsynaptic density protein (PSD95) (Fig. 4C) and Map2 was used as a neuronal marker. No difference was observed between control and GD iAstrocytes in promotion of PSD95 + /Syn1 + puncta.

3.5. The transfer of α-synuclein to iAstrocytes

In our previous study, we showed that α-syn levels were elevated in the cell body and neurites in GD1-PD and GD2 iDA neurons. Moreover, we showed co-localization of α-syn with the lysosomal marker Lamp2 in GD2 and GD1-PD cells, indicating the presence of α-syn in lysosomes (Aflaki et al., 2016). α-Syn has been described as an exogenous stimulator of astrocytes (Lee et al., 2010a). To test this, we collected conditioned medium from iDA neurons after 120 days in culture, and measured α-syn levels. Fig. 5A shows that GD2 and GD1-PD iDA neurons released the most α-syn in the medium (supernatant). Next, we tested the transmission of α-syn from iDA neurons (Fig. 5A-top panel) to iAstrocytes in a co-culture system using transwells with 0.4 μM pores. After 48 h, iAstrocytes were evaluated for the presence of α-syn by immunoblotting. iAstrocytes before co-culture showed no α-syn, as these cells do not express endogenous α-syn. However, after co-culture with iDA neurons, we observed the presence of monomeric α-syn in all iAstrocytes, indicating the transmission of α-syn from neurons to astrocytes. Furthermore, higher molecular weight α-syn was observed in the GD2 and GD1-PD iAstrocytes (Fig. 5B).

3.6. The effect of adding extrinsic α-synuclein to the iAstrocytes

Next, we treated iAstrocytes with α-syn monomers or fibrils for 48 h

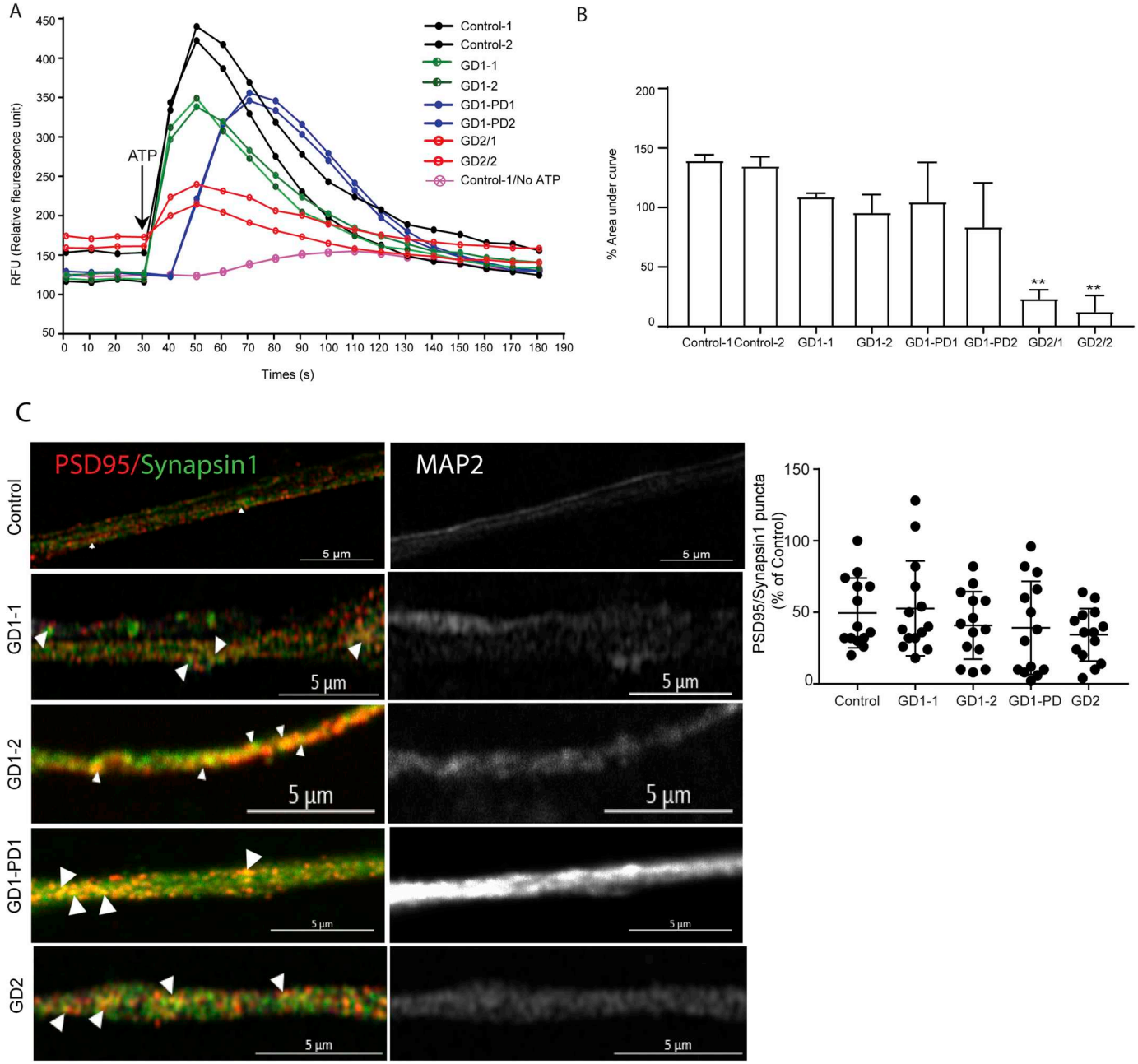

Fig. 4. .Calcium response to extracellular ATP. (A) iAstrocytes were stained with Fluo-4 AM and were stimulated with 3 µM ATP. Fluorescence at 494/516 nm was measured kinetically for 150 min. (B) Bar graph representing the % of area under curve from 4 independent experiments. (C) Images show representative neurite segments used to analyse synaptogenesis. Neurons were stained with PSD95 (red), Synapsin1 (green) and MAP2 (white). (Scale bar; 5 µm). The number of PSD95 + / Synapsin1 + puncta were analyzed (graph) using a Puncta analyzer. Data represents pooled data from two independent differentations and each experiment was repeated four times.

and lysates were immunoblotted and probed for α-syn. When treated with monomeric α-syn, iAstrocytes from only one patient, GD1-PD2 (genotype N370S/c.84insG) demonstrated increased 14 kDa α-syn, with lesser amounts of higher molecular weight α-syn (Fig. 5C). However, when fibrils were added, GD2 and GD1-PD iAstrocytes both showed significant accumulation of 14 kDa α-syn, as well as higher molecular weight α-syn (Fig. 5C). To better evaluate the accumulation of aggregated α-syn in iAstrocytes from the different patients, TR-FRET (HTRF) was performed on the lysates of iAstrocytes after treatment with monomeric and fibrillar α-syn. Fig. 5D illustrates significant increases in aggregated α-syn in GD1 and GD2 iAstrocytes in the presence of fibrils. Accumulation of aggregated α-syn after treatment with monomeric α-syn was also observed in GD1 and GD2 iAstrocytes. (Fig. 5D). To determine whether iAstrocytes prefer to accumulate α-syn or to secret it into the medium, lysates and supernatants of iAstrocytes treated with monomeric or fibrilar a-syn were evaluated by ELISA. Fig. 5E, F show accumulation of α-syn in lysates after treatment with fibrils in iAstrocytes from patients GD1-PD2 and GD2, while elevation of α-syn levels were observed in the supernatant when cells were treated with monomeric α-syn. These results indicate that GD1-PD and GD2 iAstrocytes tend to accumulate aggregated α-syn in the cells, while they secret a significant portion of the monomeric α-syn into the extracellular matrix.

To study the trafficking of α-syn in iAstrocytes, cells were treated with labeled α-syn for different time intervals, and immunofluorescence staining was performed to identify proteins associated with specific

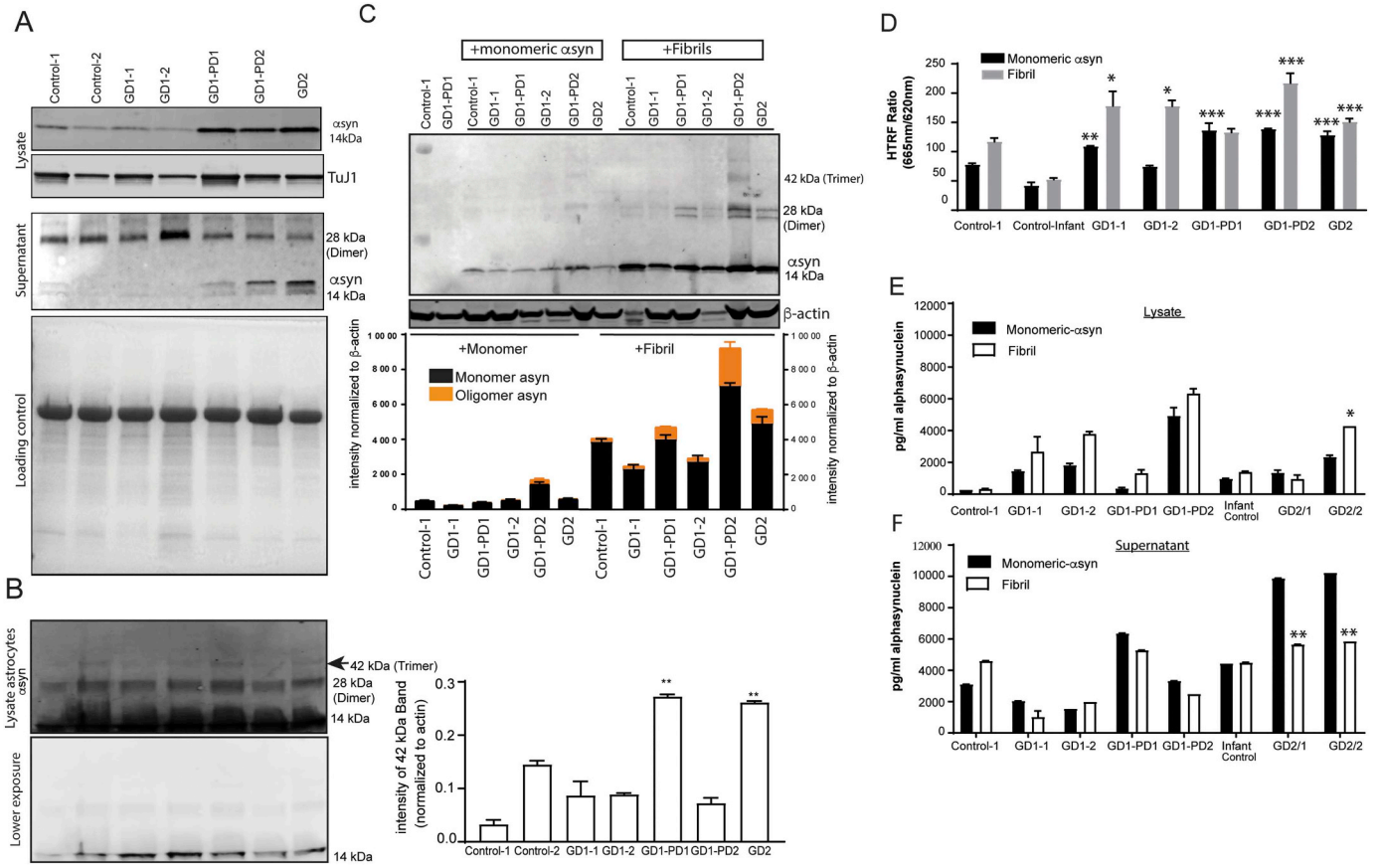

Fig. 5. Co-culture of iDopaminergic neurons with iAstrocytes. iDopaminergic neurons were co-cultured with iAstrocytes derived from the same iPSC line using transwells (0.4 μm pores). (A) The cell lysates and supernatant of (iDA) top panel and (B) cell lysates of iAstrocytes (bottom panel) were analyzed for α-syn. Coomassi-blue staining was used as the loading control for the supernatant. (C) Immunoblotting of α-syn in iAstrocytes in the presence and absence of added monomeric α-syn or fibrils. The graph represents data from two independent differentiations and four experiments. (D) iAstrocytes were treated with monomeric (*p = .02; ***p = .0001; .0003) or fibrillar (*p = .01; ***p = .0006) α-syn and HTRF was performed after a 48 h after incubation. Data represents two independent differentations and experiments were performed two times and in triplicate. (D, E) ELISA quantification of human α-syn in the lysates and supernatants of iAstrocytes after treatment with monomeric or fibrillar α-syn for 48 h. Graph represents pooled data from two independent differentiations and four experiments, each performed in triplicate.

stages of endosome maturation. Rab5, Rab7 and Rab11 are indicators of early and late endosomes, while Cathepsin D (CathD) and Lamp1 were used as lysosomal markers. Fig. 6A indicates that 24 h after α-syn internalization, most α-syn co-localized with Rab5 positive vesicles. Also, Rab7 and Rab11 levels were evaluated in iAstrocytes treated with monomeric or fibrillar α-syn. Fig. 6B–E illustrate reduced Rab7 and Rab11 in GD2 and GD1-PD iAstrocytes. Furthermore, Rab7 and Rab11 levels were increased in the presence of monomer or fibrils in control iAstrocytes, while they were unchanged in GD1-PD and GD2 iAstrocytes. Further analysis of internalized α-syn showed that labeled α-syn co-localized with the lysosomal markers Lamp2 and CathD, although CathD levels were significantly lower around labeled α-syn in GD2 iAstrocytes (Fig. 7A). We also studied the expression of Lamp2 and CathD in iAstrocytes. Lamp2 levels were increased in GD1 samples (with or without PD) and in GD2 iAstrocytes, while the ratio of mature to immature CathD was reduced significantly only in GD2 iAstrocytes (Fig. 7B, C). In addition, CathD activity was evaluated in the presence or absence of monomeric and fibrillar α-syn at acidic pH in iAstrocytes (pH 5.3). Indeed, the activity of CathD was reduced in GD2, GD1 and GD1-PD samples in the presence or absence of monomeric or fibrillar α-syn compared to control iAstrocytes (Fig. 7D).

Taken together, these data suggest that accumulation of aggregated α-syn in GD1-PD or GD2 iAstrocytes can result from the transmission of excessive α-syn from neurons. In addition, impaired endosome maturation and reduced CathD and GCase activity accelerate α-syn aggregation in the lysosomes of iAstrocytes.

3.7. α-Syn in astrocytes impacts neuroinflammation

The inflammatory response in non-stimulated iAstrocytes and those stimulated with monomeric and fibrillar α-syn was evaluated using a cytokine and chemokine proteome profiler. All non-stimulated iAstrocytes secreted MIF and SerpinE1. However, the secretion of these cytokines, as well as MCP1, were substantially increased in GD1-PD iAstrocytes and especially in GD2 iAstrocytes compared to controls.

Following a 48 h exposure to endotoxin-free monomeric α-syn, MIF and Serpin E1 levels increased in all iAstrocytes. We specifically observed secretion of MCP1, CXCL1 and IL-8 in GD1-PD iAstrocytes, increased MCP1 levels in GD1 iAstrocytes and enhanced CXCL1 and IL-6 secretion in GD2 iAstrocytes (Fig. 8). The iAstrocytes also were also treated with fibrils, resulting in MIF and Serpin E1 secretion in control, GD1 and GD1-PD iAstrocytes. While there was MCP1 and IL-6 secretion in control iAstrocytes, CXCL1 and IL-8 secretion was seen in GD1-PD iAstrocytes. Interestingly, IL-8, CXCL1 and MCP1 secretion were observed in GD2 iAstrocytes exposed to fibrillar α-syn.

4. Discussion

While there has been neuropathological evidence that astrocytes play a role in neuronopathic GD, very few studies have focused on the

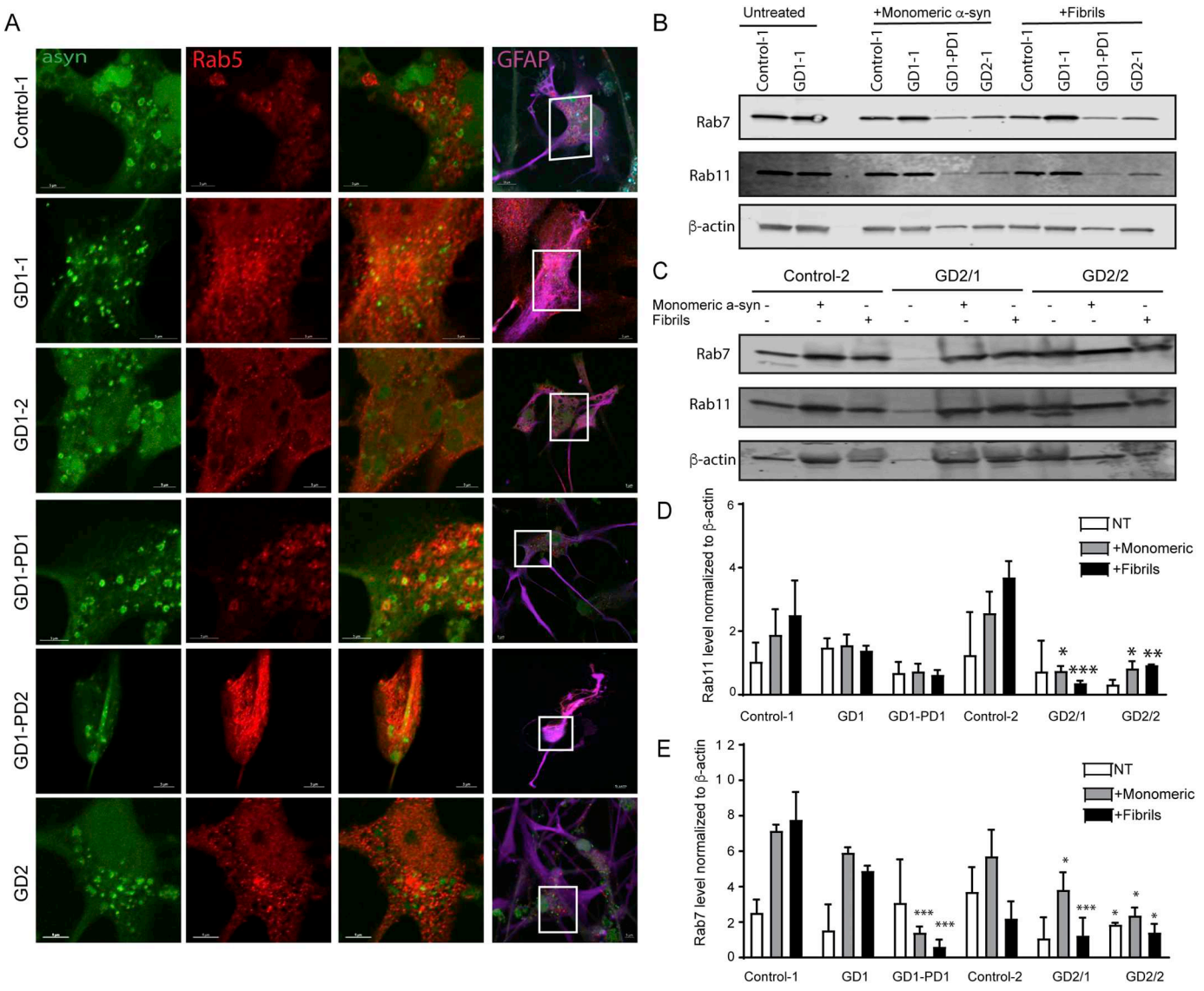

Fig. 6. Trafficking of labeled-α-syn in iAstrocytes. (A) iAstrocytes were treated with labeled α-syn (green) for 24 h, and then fixed and stained for Rab5 (red) and GFAP (purple). *Z*-stack images were acquired using a Zeiss 880 confocal microscope (63× magnification). Insets, Higher magnification of the areas outlined in the images as shown. Scale bars; 5 μm. (B, C) Western blot analysis of Rab7 and Rab11 levels in iAstrocytes in the presence or absence of monomeric or fibrillar α-syn for 48 h. β-actin was used as the loading control. (D, E) Quantification of Rab7 (*$p = .026$; ***$p = .0001$) and Rab11 (**$p = .002$; ***$p = .0002$) levels in iAstrocytes in the presence and absence of monomer or fibril α-syn. Experiments were perfomed from 2 ineipendent differentiations.

effect of GCase deficiency on astrocytes. Moreover, many aspects of the pathogenesis of GD remain a puzzle, as the degree of neuropathology observed in type 2 GD does not seem to correlate with the extreme, progressive and early phenotype of these infants. Our recent ability to generate iAstrocytes from different patient fibroblasts provides a new means to explore the role of this interesting and abundant cell type. Transcriptome data from human astrocytes and human neurons show that more GCase is expressed in astrocytes than neurons (Zhang et al., 2016). A careful neuropathological analysis of selected brain regions in brain autopsy samples from 14 patients with different types of GD by Wong et al. (Wong et al., 2004) demonstrated that patients with GD2 showed astrogliosis with prominent neuronal loss, whereas those with GD1 had only mild astrogliosis, without neuronal loss.

In this study, we show that iAstrocytes from patients with GD1 (with or without PD), manifest mild to moderate astrogliosis and mildly up-regulated GFAP, but no cell proliferation. In contrast, iAstrocytes from patients with GD2 show severe diffuse astrogliosis, as reflected by increased GFAP levels, cytoskeleton hypertrophy and increased cell proliferation. Importantly, GD2 iAstrocytes exhibited decreased expression of the water channel, Aquaporin-4, which is involved in blood-brain-barrier function and water transport (Nagelhus and Ottersen, 2013). Aquaporin 4 also is involved in the migration of astrocytes, which might be very important in the progression of neurodegenerative disease.

We preiously showed that the glucosylsphingosine levels in brain samples from patients with type 2 GD were significantly higher than those in control and GD1 brain samples (Orvisky et al., 2002). Our current data shows that iAstrocytes recapitulate this finding, for while GluSph levels were barely detectable in control and GD1 iAstrocytes, the levels were significantly higher in GD2 iAstrocytes. These data suggest that in GD2, GlcSph-rich astrocytes may contribute to disease progression by exposing the brain to toxic levels of GlcSph, which cannot be degraded by GCase.

Recently our group has shown accumulation of α-syn in iPS-derived dopaminergic neurons from patients with GD2 and GD1/PD (Aflaki et al., 2016). Although α-syn accumulation is primarily seen in neurons, it can also be detected in astrocytes (Braak et al., 2007; Wakabayashi et al., 2000). While it has been shown that iAstrocytes from patients

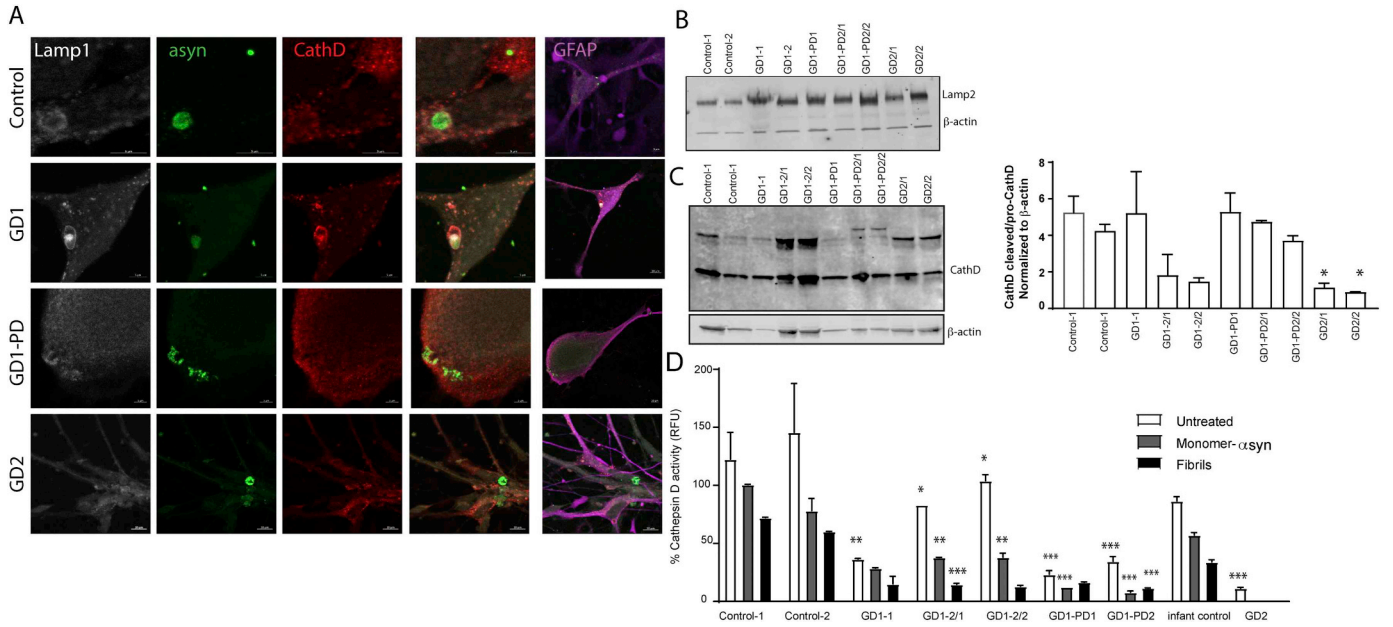

Fig. 7. Cathepsin D in iAstrocytes. (A) iAstrocytes were treated with labeled α-syn (green) for 48 h and then stained for CathD (red), Lamp1 (white) and GFAP (purple). (B) Western blot analysis of Lamp2 in iAstrocytes from control, GD1, GD1-PD and GD2 iAstrocytes, β-actin was used as the loading control. (C) Immunoblot analysis of CathD levels in iAstrocytes. The graph represents CathD levels measured from two independent differentiations (*p = .008). (D) CathD activity in iAstrocytes in the presence and absence of monomeric and fibrillar α-syn, measured in two independent differentiations and pooled data from four different experiments (*p = .026; **p = .008; ***p = .0001, .0006).

with PD carrying the G2019S mutation in *LRRK2* have impaired macroautophagy and extensive α-syn accumulation (di Domenico et al., 2019). the possible contribution of α-syn inclusions in astrocytes to the progression of neurodegenerative disorders like neuronopathic GD and *GBA1*-associated PD has not been studied. The importance of astrocytes in disease progression is largely dependent on the uptake and release of substances that they receive from neurons, such as engulfed dead cells, synapses and α-syn (Danzer et al., 2011; Loov et al., 2012; Sofroniew

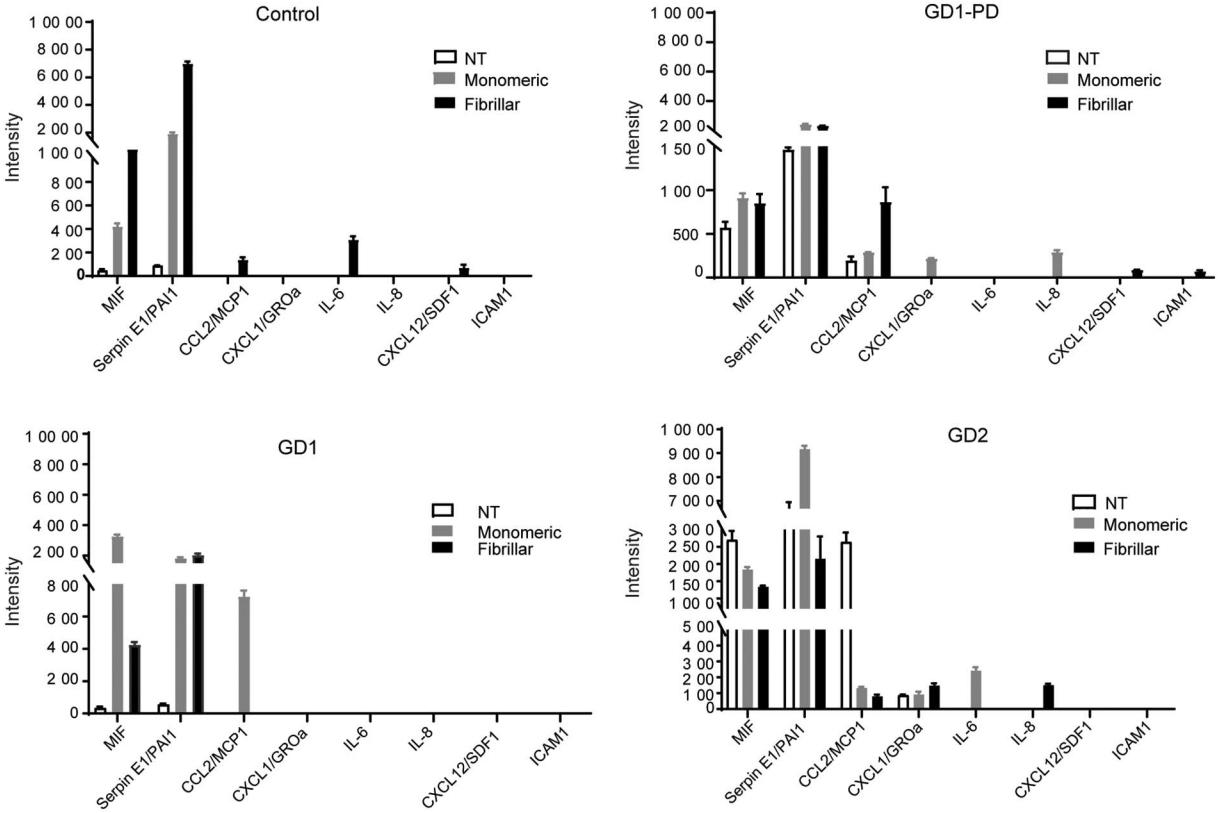

Fig. 8. Proteome profiler array of cytokines/chemokines in iAstrocytes. Levels of secreted cytokines and chemokines measured in control, GD1, GD1-PD and GD2 iAstrocytes stimulated with monomeric or fibullar α-syn for 48 h.

and Vinters, 2010). Furthermore, it has been shown that a-syn can be taken up by astrocytes via endocytosis, which can explain the role of astrocytes in the removal of excessive α-syn secreted by neurons (Lee et al., 2010b). Our co-culture experiments using different iPSC-derived lineages from the same individual demonstrate that excessive α-syn transfers from dopaminergic neurons to iAstrocytes. Generally, control and GD1 iAstrocytes secret the α-syn into the extracellular matrix. However, in GD2 and GD1-PD iAstrocytes, α-syn was found in the lysosomes, where it co-localized with the lysosmal marker LAMP2. Levels of aggregated α-syn increased significantly in these cells when they were treated with monomeric and fibrillar α-syn. This appears to result from impaired endosomal maturation in GD1-PD and GD2 iAstrocytes, as reflected by reduced expression of Rab11b. Moreover, in the GD2 iAstrocytes, cathepsin D activity and its translocation were impaired.

In summary, in both GD1-PD and GD2 iAstrocytes, α-syn is secreted from dopaminergic neurons, is endocytosed by astrocytes and is translocated to the lysosome for degradation. If the concentration of α-syn is increased significantly, this leads to the accumulation of α-syn in the lysosome, which is compounded by compromised α-syn degradation due to diminished cathepsin D activity.

We then explored the potential impact of the presence of aggregated α-syn in astrocytes on neuroinflammation. Choi et al (Choi et al., 2014) showed the expression of eight cytokines in non-stimulated human astrocytes isolated from brain tissue and cultured in 10% FBS including, G-CSF, G-MCSF, CXCL1, IL-6, IL-8, MCP1, MIF and Serpin E1. For the first time, we show that both non-stimulated and stimulated iAstrocytes secret MIF and Serpin E1, and that the levels of these cytokines are elevated significantly in GD2 and GD1-PD iAstrocytes. MCP1 secretion, which was not observed in control or GD1 iAstrocytes, was found in the stimulated iAstrocytes secretome of GD2 and GD1-PD iAstrocytes. Together, these data indicate that the secretion of the inflammatory cytokines IL-6, CXCL1 and IL-8 increase following exposure to monomeric α-syn.

In conclusion, our study shows the importance of active astrocytes and their role in the progression of neurodegenerative diseases like PD and the acute neuronopathic form of GD. Astrocytes appear early in embryonic development and play critical roles in neuronal survival. GD2 iAstrocytes are both morphologically and functionally impaired, and likely contribute to the devastating neurodegenerative course observed in this disease. In addition, GD/PD iAstrocytes show impaired processing of α-syn and neuroinflammation. Since iAstrocytes are relatively hearty and easy to grow, they serve as an important cellular model for studies of disease pathogenesis that can be used to facilitate drug development.

Acknowledgements and funding

This research was supported by the Intramural Research Program of the National Human Genome Research Institute and the National Institutes of Health. The authors acknowledge Dr. Cindy McKinney for her helpful comments.

References

Aflaki, E., et al., 2014. Macrophage models of Gaucher disease for evaluating disease pathogenesis and candidate drugs. Sci. Transl. Med. 6, 240ra73.
Aflaki, E., et al., 2016. A new glucocerebrosidase chaperone reduces alpha-synuclein and glycolipid levels in iPSC-derived dopaminergic neurons from patients with Gaucher disease and parkinsonism. J. Neurosci. 36, 7441–7452.
Allen, N.J., 2014. Synaptic plasticity: astrocytes wrap it up. Curr. Biol. 24, R697–R699.
Belanger, M., Magistretti, P.J., 2009. The role of astroglia in neuroprotection. Dialogues Clin. Neurosci. 11, 281–295.
Braak, H., et al., 2007. Development of alpha-synuclein immunoreactive astrocytes in the forebrain parallels stages of intraneuronal pathology in sporadic Parkinson's disease. Acta Neuropathol. 114, 231–241.
Choi, S.S., et al., 2014. Human astrocytes: secretome profiles of cytokines and chemokines. PLoS One 9, e92325.
Chung, W.S., et al., 2013. Astrocytes mediate synapse elimination through MEGF10 and MERTK pathways. Nature. 504, 394–400.
Danzer, K.M., et al., 2011. Heat-shock protein 70 modulates toxic extracellular alpha-synuclein oligomers and rescues trans-synaptic toxicity. FASEB J. 25, 326–336.
DeSilva, T.M., et al., 2012. Expression of EAAT2 in neurons and protoplasmic astrocytes during human cortical development. J. Comp. Neurol. 520, 3912–3932.
di Domenico, A., et al., 2019. Patient-specific iPSC-derived astrocytes contribute to non-cell-autonomous neurodegeneration in Parkinson's disease. Stem Cell Rep. 12, 213–229.
Du, F., et al., 2018. Astrocytes attenuate mitochondrial dysfunctions in human dopaminergic neurons derived from iPSC. Stem Cell Rep. 10, 366–374.
Eid, T., et al., 2005. Loss of perivascular aquaporin 4 may underlie deficient water and K + homeostasis in the human epileptogenic hippocampus. Proc. Natl. Acad. Sci. U. S. A. 102, 1193–1198.
Halassa, M.M., et al., 2007. The tripartite synapse: roles for gliotransmission in health and disease. Trends Mol. Med. 13, 54–63.
Ippolito, D.M., Eroglu, C., 2010 Nov. Quantifying synapses: an immunocytochemistry-based assay to quantify synapse number. J. Vis. Exp. 16 (45), 2270. https://doi.org/10.3791/2270. (21113117).
Jakes, R., et al., 1994. Identification of two distinct synucleins from human brain. FEBS Lett. 345, 27–32.
Johnson, M., et al., 2010. Targeted amino-terminal acetylation of recombinant proteins in *E. coli*. PLoS One 5.
Lee, R.E., 1982. The pathology of Gaucher disease. Prog. Clin. Biol. Res. 95, 177–217.
Lee, H.J., et al., 2010a. Alpha-synuclein stimulation of astrocytes: potential role for neuroinflammation and neuroprotection. Oxidative Med. Cell. Longev. 3, 283–287.
Lee, H.J., et al., 2010b. Direct transfer of alpha-synuclein from neuron to astroglia causes inflammatory responses in synucleinopathies. J. Biol. Chem. 285, 9262–9272.
Lin, L.F., et al., 1993. GDNF: a glial cell line-derived neurotrophic factor for midbrain dopaminergic neurons. Science 260, 1130–1132.
Loov, C., et al., 2012. Engulfing astrocytes protect neurons from contact-induced apoptosis following injury. PLoS One 7, e33090.
Masuda, M., et al., 2006. Cysteine misincorporation in bacterially expressed human alpha-synuclein. FEBS Lett. 580, 1775–1779.
Nagelhus, E.A., Ottersen, O.P., 2013. Physiological roles of aquaporin-4 in brain. Physiol. Rev. 93, 1543–1562.
Nalls, M.A., et al., 2013. A multicenter study of glucocerebrosidase mutations in dementia with Lewy bodies. JAMA Neurol. 70, 727–735.
Nielsen, S., et al., 1997. Specialized membrane domains for water transport in glial cells: high-resolution immunogold cytochemistry of aquaporin-4 in rat brain. J. Neurosci. 17, 171–180.
O'Leary, E.I., et al., 2018. Effects of phosphatidylcholine membrane fluidity on the conformation and aggregation of N-terminally acetylated alpha-synuclein. J. Biol. Chem. 293, 11195–11205.
Orvisky, E., et al., 2002. Glucosylsphingosine accumulation in tissues from patients with Gaucher disease: correlation with phenotype and genotype. Mol. Genet. Metab. 76, 262–270.
Pfefferkorn, C.M., Lee, J.C., 2010. Tryptophan probes at the a-synuclein and membrane interface. J. Phys. Chem. B 114, 4615–4622.
Phatnani, H., Maniatis, T., 2015. Astrocytes in neurodegenerative disease. Cold Spring Harb. Perspect. Biol. 7.
Segura-Aguilar, J., 2015. A new mechanism for protection of dopaminergic neurons mediated by astrocytes. Neural Regen. Res. 10, 1225–1227.
Serio, A., et al., 2013. Astrocyte pathology and the absence of non-cell autonomy in an induced pluripotent stem cell model of TDP-43 proteinopathy. Proc. Natl. Acad. Sci. U. S. A. 110, 4697–4702.
Sidransky, E., et al., 2009. Multicenter analysis of glucocerebrosidase mutations in Parkinson's disease. N. Engl. J. Med. 361, 1651–1661.
Sofroniew, M.V., Vinters, H.V., 2010. Astrocytes: biology and pathology. Acta Neuropathol. 119, 7–35.
Tu, P.H., et al., 1998. Glial cytoplasmic inclusions in white matter oligodendrocytes of multiple system atrophy brains contain insoluble alpha-synuclein. Ann. Neurol. 44, 415–422.
Wakabayashi, K., et al., 2000. NACP/alpha-synuclein-positive filamentous inclusions in astrocytes and oligodendrocytes of Parkinson's disease brains. Acta Neuropathol. 99, 14–20.
Wong, K., et al., 2004. Neuropathology provides clues to the pathophysiology of Gaucher disease. Mol. Genet. Metab. 82, 192–207.
Zhang, Y., et al., 2016. Purification and characterization of progenitor and mature human astrocytes reveals transcriptional and functional differences with mouse. Neuron. 89, 37–53.